# Unorthodox Interactions at Work

Yingjie Zhao,[†] Yoann Cotelle, Naomi Sakai, and Stefan Matile*

Department of Organic Chemistry, University of Geneva, CH-1211 Geneva, Switzerland

**ABSTRACT:** This Perspective elaborates on the currently unfolding interest in integrating unorthodox non-covalent interactions into functional systems. Initial emphasis is on anion−$\pi$ interactions at work, particularly in catalysis. Recent highlights are described in comparison to a coinciding renaissance of the more conventional, charge-inverted cation−$\pi$ catalysis. Progress with these complementary aromatic systems is then compared to recent efforts to integrate halogen and chalcogen bonds, the unorthodox counterparts of hydrogen bonds, into functional systems. General focus is on catalysis, pertinent examples on self-assembly, transport, sensing, and templation are covered as well.

## 1. INTRODUCTION

The use of unorthodox interactions to construct and operate functional systems attracts increasing attention. This is understandable because the discovery of conceptually innovative ways to create function promises to advance the chemical sciences in the most fundamental manner. The term "unorthodox" certainly depends on the circumstances. For example, cation−$\pi$ interactions are very well recognized by now, but their explicit integration into the rational design of new catalysts remains remarkably rare and recent.[1−4] In this Perspective, we focus exclusively on experimental insights in support of the functional relevance of non-covalent unorthodox interactions. Initial emphasis is on anion−$\pi$ interactions[5−10] in comparison to cation−$\pi$ interactions,[1−4,11] their more conventional counterpart. Applying lessons from binding, transport, sensing as well as biosynthesis, their current integration into catalysis is motivated by the general idea to stabilize anionic and cationic transition states on $\pi$-acidic and $\pi$-basic aromatic surfaces, respectively. This unorthodox chemistry on aromatic surfaces is then connected to coinciding developments with halogen bonds,[12−19] the unorthodox counterpart of hydrogen bonds, and with chalcogen bonds,[20−23] the equally underexplored homologue of halogen bonds. Operating with $\sigma$ holes rather than $\pi$ holes,[24] halogen and chalcogen bonds are of interest in functional systems because of their exceptional directionality, their strength and their overall low polarity. The objective of this Perspective is to bundle and compare these simultaneous recent developments toward unorthodox interactions that work, particularly in catalysis.

## 2. ANION−$\pi$ INTERACTIONS AT WORK

The term "anion−$\pi$ interaction" refers to the binding of anions on the $\pi$ surface of aromatic systems, with distances around or preferably shorter than the sum of the individual vdW radii.[24−26] In analogy to cation−$\pi$ interactions, this definition refers to the site of the interaction, in principle without any implications on their nature. This theoretical understanding is quite complex, still under debate and well beyond the topic of this Perspective. However, there is fairly general agreement that anion−$\pi$ interactions require $\pi$-acidic aromatic systems with positive quadrupole moment $Q_{zz}$, whereas conventional $\pi$ bases with negative $Q_{zz}$ attract cations. Both interactions are strengthened by contributions from induced dipoles perpendicular to the $\pi$ plane and permanent in-plane dipoles from electron donating or accepting substituents (graphical abstract).

Complementary to cation−$\pi$ interactions, anion−$\pi$ interactions relate to LUMO chemistry. Overperforming anion−$\pi$ interactions produce charge-transfer complexes and radicals, a behavior that is comparable to proton transfer between conjugate acids and bases with "too strong" hydrogen bonds. Alternatively, "too strong" anion−$\pi$ interactions can result in $\sigma$ complexes and nucleophilic aromatic substitution, whereas the complementary cation−$\pi$ interactions can proceed to electrophilic aromatic substitution. As with cation−$\pi$ interactions, anion−$\pi$ interactions can appear mixed up with other interactions such as ion pairing or $\pi$−$\pi$ interactions. Such contributions are involved in the still relatively pure nitrate−$\pi$ or enolate−$\pi$ interactions and more significantly in dimers or $\pi$ stacks that integrate charged aromatic components or with anions on the surface of cationic aromatics. Catalysis, with charges moving on $\pi$ surfaces, naturally enters this greyzone beyond the pure, ideal interaction with a spherical ion localized on the center of an aromatic ring.

Compared to the established cation−$\pi$ interactions, anion−$\pi$ interactions are much younger. Considered occasionally before,[27] anion−$\pi$ interactions have been introduced explicitly, based on positive $Q_{zz}$, by theoreticians in 2002. Observed by now in solid, solution and gas phase,[24−26] anion−$\pi$ interactions appeared first in functional systems only 10 years ago.[28] Today, transport with anion−$\pi$ interactions is almost routine and attention is shifting toward self-assembly on the one hand[9,10] and catalysis on the other.[4−8] The current emergence of anion−$\pi$ catalysis coincides with a renaissance of the complementary, still surprisingly underexplored cation−$\pi$ catalysis,[1−4] and with pioneering studies on catalysis mediated by halogen[12−17] and chalcogen bonds.[20,21]

**2.1. Cation−$\pi$ Catalysis.** Experimental evidence that anion−$\pi$ interactions could stabilize anions in the ground state during transport implied that they could also be of use in catalysis.[29] There was no reason to believe why lessons from transport could not be applied to the stabilization of anionic intermediates and transition states on $\pi$-acidic surfaces. Moreover, the complementary, conventional cation−$\pi$ inter-
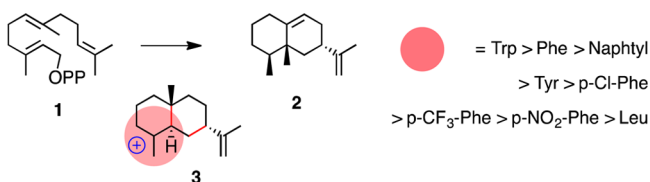
**Figure 1.** The yield of aristolochene **2** increases linearly with the $\pi$ basicity of the amino-acid residue in the enzyme that stabilizes the cationic eudesmane intermediate **3** (red circle).



**Figure 3.** Retention of configuration during the nucleophilic substitution from (S)-**15** to (S)-**16** is thought to originate the stereoselective stabilization of reactive intermediate **TS2** by cation–$\pi$ interactions within the supramolecular catalyst **14**.

actions are very well known to catalyze key reactions in biosynthesis (Figure 1). Most spectacular is the stabilization of carbocation intermediates by a cluster of $\pi$-basic amino acid residues during the cascade cyclization of 2,3-squaleneoxide into steroids.[30] A related recent example from biosynthesis concerns the cyclization of farnesylpyrophosphate **1** into aristolochene **2**.[11] The $\pi$-basic residue expected to stabilize the intermediate eudesmane carbocation **3** was systematically replaced by artificial amino acids with different $\pi$ acidity. Increasing yield of aristolochene with decreasing $\pi$ acidity of the eudesmane-stabilizing residue confirmed the occurrence of cation–$\pi$ catalysis.

Considering the importance of cation–$\pi$ enzymes in biosynthesis, particularly terpenoid cyclizations, it is surprising to realize that cation–$\pi$ interactions did not receive much attention in organocatalysis so far. Proof-of-principle has been available since the early 1990s.[31] The recent renaissance of cation–$\pi$ interactions in organocatalysis has arguably been triggered by the marvelous biomimetic cascade cyclization of substrate **4** into **5** (Figure 2).[1] The original catalyst **6** contains a thiourea to bind the anionic leaving group OH⁻. The resulting carbocation then engages in a cascade cyclization toward product **5**, as outlined in **TS1** (transition state 1). The stereoselectivity of this cascade process increases with increasing size, polarizability and $\pi$ basicity of the aromatic $\pi$ surface in catalysts **6–9**. This almost linear dependence was considered as decisive experimental evidence that the stabilization of the carbocation intermediates with cation–$\pi$ interactions during the cascade cyclization from **4** to **5** is as essential as in similar cascades during terpenoid biosynthesis.

In a most recent highlight, the capsule **10**₆ ($H_2O$)₈, formed by self-assembly of resorcinarene **10**, is introduced as cation–$\pi$ catalyst.[2] The high Brønsted acidity within this capsule catalyzes the formation of an allylic carbocation from nerol **11**. Stabilized by cation–$\pi$ interactions within the capsule, this carbocation then cyclizes first into $\alpha$ terpineol **12** and then into the bicyclic eucalyptol **13**. Without the capsule, these reactions
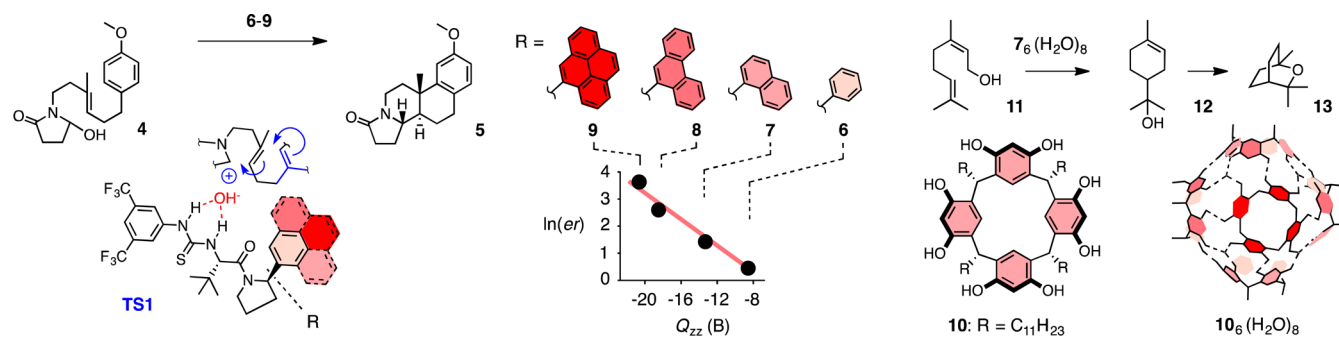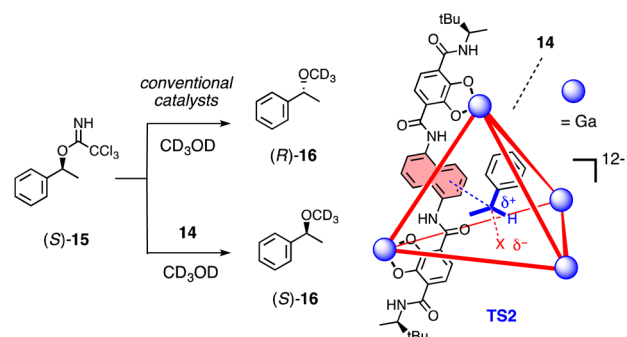
do not occur selectively, more complex product mixtures are usually observed. The same capsule has been used before for cation–$\pi$ catalysis of selective Wittig reactions and acetal hydrolysis.[32]

Similar monoterpene cyclizations have been achieved with supramolecular catalysts such as **14** (Figure 3).[33] These tetrahedral, highly anionic architectures are constructed by coordination of catecholate ligands to gadolinium cations. Another reaction catalyzed by the supramolecular capsule **14** is the solvolysis of enantiopure substrate (S)-**15** with up to 74% retention of configuration.[3] This is remarkable because conventional catalysts afford product (R)-**16** with up to 84% inversion of configuration as expected for an $S_N2$ reaction. The unexpected stereoselectivity of the supramolecular catalyst **14** has been rationalized by the stabilization of the increasing positive charge on the benzylic carbon in **TS2** by cation–$\pi$ interactions with the $\pi$-basic naphthalenes of the capsule.

The MacMillan catalyst **17**[34] has been suspected early on to operate with cation–$\pi$ interactions (Figure 4).[35] This intriguing hypothesis could recently be validated with a systematic study using the Friedel–Crafts alkylation of methylpyrrole **18** as model reaction.[4] In this process, enone **19** first reacts with the catalyst to form an iminium intermediate. This covalent intermediate then reacts with the methylpyrrole **18** as outlined in **TS3** and **TS4**. Subsequent aldehyde reduction affords product **20**. To assess the possible stabilization of the iminium intermediate by cation–$\pi$ interactions, catalysts **21–23** were prepared. With increasingly negative quadrupole moment of the $\pi$ base in the catalyst, the stereoselectivity of the reaction increased. This stereoselective Friedel–Crafts alkylation also provides a great illustration of the notion developed in the
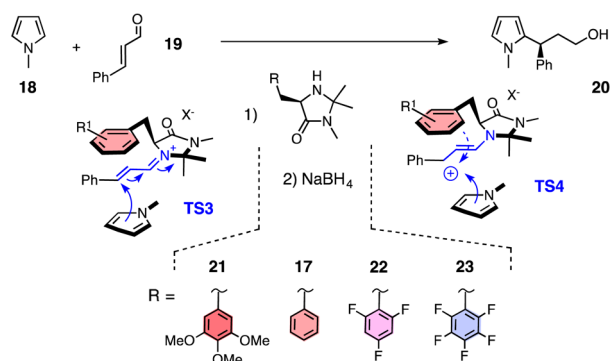


**Figure 2.** Cascade cyclizations with carbocation intermediates catalyzed by the recent cation–$\pi$ catalysts **6-10**, with indication of the dependence of stereoselectivity of the reaction on the quadrupole moment of the cation–$\pi$ catalysts.

**Figure 4.** Stereoselectivity of the Friedel−Crafts alkylation decreases with increasing $\pi$ acidity of cation−$\pi$ catalysts **17** and **21**−**23**. **TS4** highlights the difference between cation−$\pi$ interactions with $\pi$ bases that do (solid arrow) and do not (dashed arrow) continue with an electrophilic aromatic substitution.

introduction that "too strong" cation−$\pi$ interactions can result in electrophilic aromatic substitution: Whereas the $\pi$ bases in the catalysts just interact, the more $\pi$-basic substrate **18** reacts (compare **TS4**, dashed vs solid arrow).

**2.2. Anion−$\pi$ Catalysis.** The first report on anion−$\pi$ catalysis appeared in 2013.[5] Extensively used for conceptual innovation in catalysis, the Kemp elimination was selected as simplest possible model reaction to elaborate on the concept (Figure 5). The key to success was the covalent positioning of a
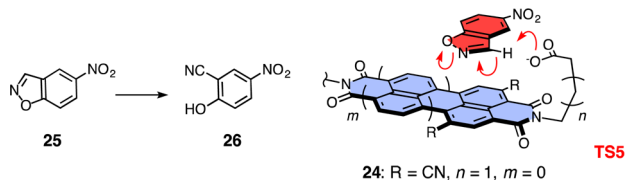


**Figure 5.** Transition-state stabilization of the Kemp elimination increases with increasing $\pi$ acidity of anion−$\pi$ catalysts (R = H, CN (**24**), SEt, SOEt, $m = 0$, $n = 1$).

weak carboxylate base on the $\pi$-acidic surface of either a naphthalenediimide (NDI, $m = 0$) or a perylenediimide (PDI, $m = 1$).[5,36] In the resulting bifunctional catalysts such as **24**, anion−$\pi$ interactions could turn on during deprotonation of substrate **25** to stabilize the single anionic transition state **TS5** as soon as the negative charge is injected into the substrate. Proton transfer to the obtained phenolate then causes the release of the repulsive product **26** and restores the carboxylate in the catalyst. Fortunately, the kinetics observed for the Kemp elimination showed Michaelis−Menten behavior. This was

important to extract absolute values for ground- and transition-state stabilization by anion−$\pi$ interactions. Best results were obtained with NDI catalysts such as **24** with cyano or sulfoxide acceptors in the core and concise Leonard turns ($n = 1$) to place the carboxylate on the $\pi$-acidic surface. Transition-state recognition calculated to $K_{TS} = 4.9\ \mu M$ (!) or $\Delta G_{TS} = -28.3$ kJ mol$^{-1}$, ground-state recognition to $K_M = 56.5$ mM or $\Delta G_{GS} = -7.1$ kJ mol$^{-1}$. Most importantly, transition-state stabilization increased with increasing $\pi$ acidity of the aromatic surface.

To explore anion−$\pi$ catalysis with more significant reactions, the addition of malonic acid half thioesters (MAHTs) **27** to enolate acceptors such as nitroolefins **28** was selected (Figure 6).[6] This enolate chemistry represents one of the most important anionic reactive intermediate in chemistry and biology. With the Claisen condensation between acetyl-CoA and malonyl-CoA, MHT addition marks the beginning of all biosynthesis and is then repeated most impressively in polyketide synthesis. Interestingly, in solution without enzymes, the addition of MAHTs **27** to enolate acceptors such as **28** is not favored. Decarboxylation products such as **29** are obtained as main products instead of the desired addition products **30**. The selectivity between the two competing reactions is possibly controlled on the level of MHT tautomers.

The tautomer in **TS6** can decarboxylate (solid arrows) before addition (dashed arrows), whereas the tautomers in **TS7** or **TS8** have to react before decarboxylation. To sense the subtle difference between these anionic tautomers—charge-delocalized planar forms against charge-localized nonplanar forms—$\pi$-acidic surfaces appeared well-suited. Anion−$\pi$ tweezers **31** or **32** with a central tertiary amine as base catalyst were already sufficient to overcome the preference for decarboxylation product **29**. Increasing $\pi$ acidity in anion−$\pi$ tweezers **33** and **34** caused an inversion of selectivity. A disfavored/favored relative yield changing from $\eta^{d/f} = 0.6$ for controls to $\eta^{d/f} = 1.9$ for tweezers **34** supported that anion−$\pi$ interactions can selectively accelerate the disfavored yet relevant reaction. Reaction kinetics indicated that the origin of this inversion of selectivity is twofold: With increasing $\pi$ acidity, i.e., lower $E_{LUMO}$ of the catalyst, the favored decarboxylation decelerates ($\Delta E_a^f > 0$), whereas the intrinsically disfavored enolate addition accelerates ($\Delta E_a^d < 0$, Figure 6, right). Most recent results on this system include the introduction of rigidified Leonard turns between $\pi$ surface and amine base (providing access to $\eta^{d/f} = 4.3$), the interfacing with more complex systems (providing access to enantioselectivity), covalent macrodilactones to systematically characterize enolate−$\pi$ interactions (increasing acidity by up to $\Delta pK_a = 5.5$), and the application to more demanding cascade processes.[37]
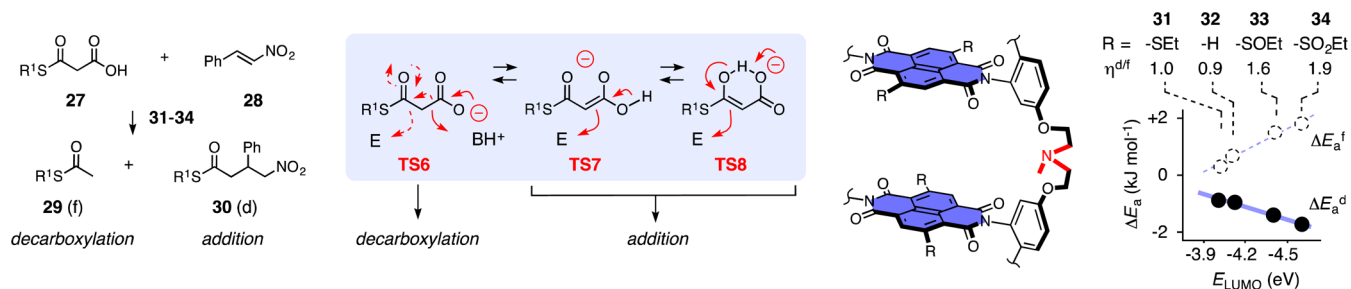


**Figure 6.** Anion−$\pi$ catalysts **31**−**34** for the selective acceleration of the intrinsically disfavored (d) but biological most relevant addition of malonates **27** to enolate acceptors such as **28**.
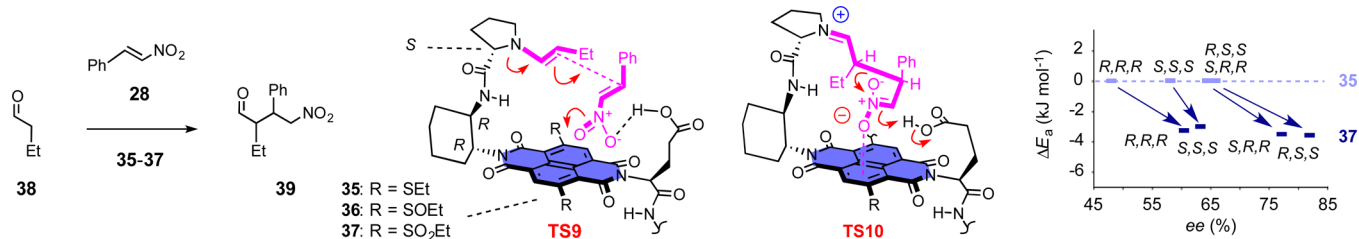
**Figure 7.** In asymmetric anion−π catalysis with trifunctional systems 35−37, rates and enantioselectivity of enamine addition to nitroolefins increase with the π acidity of the catalysts.

Asymmetric anion−π catalysis was realized first with enamine chemistry (Figure 7).[7] In catalysts 35−37, a proline is placed at some distance at one side of the π-acidic surface, and a glutamate in close proximity at the other side. Enamine formation then prepares for the addition of aldehyde 38 to nitroolefin 28 (TS9). Subsequent proton transfer from the proximal acid to the nitronate intermediate shifts the rate-limiting step from TS10 to C−C bond formation in TS9. This design assures that the reaction occurs on the π-acidic surface (esterification inactivated the trifunctional catalysts). With increasing π acidity from 35 to 37, both rate and stereo-selectivity of the reaction increased, independent of the configuration on the proline side (Figure 7, right side; the glutamate was kept constant). Results with catalysts 36 were more complex because of the additional stereogenic centers of the sulfoxides at the edge of the π surface. However, with perfectly matched, fully rigidified architectures, catalysts 36 with chiral π surfaces afforded product 39 with highest rate, enantioselectivity, and diastereoselectivity.

Contributions of anion−π interactions to anion-binding catalysis have been suggested recently.[8] Chloride elimination from substrate 40 (TS11) followed by addition of the resulting carbocation to silyl enol ether 41 gives ester 42 (Figure 8). This transformation has been introduced as model reaction to probe for anion-binding catalysis. In catalyst 43, anion binding is accomplished by an electron-deficient pyridinium cation. Anion−π interactions with the pentafluorobenzyl substituent have been confirmed to occur in solid and solution. However, catalytic activity of pentafluorobenzyl catalyst 43 did not differ much from other withdrawing substituents such as cyanomethyl.

In nature, anion−π catalysis is almost absent because strongly π-acidic aromatics exist neither in proteins nor in nucleic acids. However, intriguing exceptions from this rule have been identified recently.[24]

With regard to both anion−π and cation−π catalysis, the role of the counterion deserves special attention. Ion pairs near aromatic systems are ubiquitous in nature and have been explored theoretically and experimentally in several elegant model systems.[38] However, the aromatic systems involved are usually too small 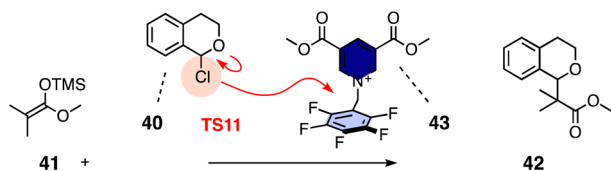and too π-basic to bind both ions on their surface. Usually, the anion is left on the side. Most recently, ion pair−π interactions have been introduced to accommodate both, the anion and the cation, on polarized push−pull π surfaces.[39] Significant contributions to the spectral tuning of push−pull chromophores and the activation of cell-penetrating peptides have been identified. Applications to catalysis have so far not been reported.

**2.3. Self-Assembly with Anion−π Interactions.** Pioneering studies on anion−π interactions at work have appeared recently also with regard to self-assembly. Anion−π interactions with the neutral tetraoxacalix[2]arene[2]triazine 44 have been studied in much detail (Figure 9).[26] As with many other architectures, nitrate−π (or in catalysis, nitronate−π) inter-actions were found to be particularly favorable. Very recently, the formation of supramolecular amphiphiles has been explored with the macrocyclic π acid 44 and hydrophobic anions such as sodium dodecyl sulfate (SDS, 45), laurate, and so on.[9] In water, the obtained supramolecular amphiphiles were found to self-assemble into vesicles. Control experiments revealed that macrocycles with donating amines in place of the chloro substituents in 44 form neither micelles nor vesicles. Moreover, the addition of competing anions such as $NO_3^-$, $Cl^-$ and $Br^-$ caused the disassembly of the vesicles and release of their content. Vesicle disassembly was also observed upon protonation of the anions in the supramolecular amphiphiles. These results have been interpreted as experimental support for contributions of anion−π interactions to self-assembly.

Another indication for contributions of anion−π interactions to self-assembly has been observed with NDI trimers 46.[10] These chiral macrocycles offer a π-acidic cavity for the inclusion of anions. The inclusion of $I_3^-$ initiated the self-assembly of NDI trimers 46 into chiral helices. The structure of these supramolecular anion−π helices has been resolved by X-ray crystallography.
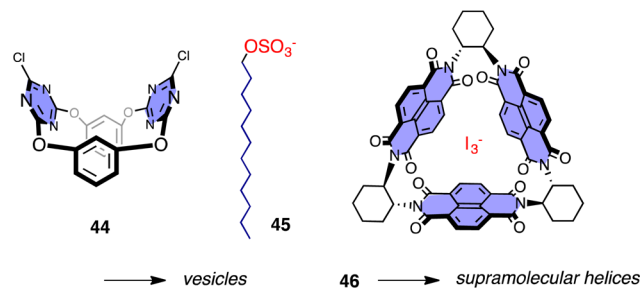


**Figure 8.** Anion-binding catalysis with possible contributions from anion−π interactions.



**Figure 9.** Self-assembly of macrocycles 44 and 46 into vesicles and helices in the presence of anions 45 and $I_3^-$, respectively.

## 3. HALOGEN BONDS AT WORK

Similar to the relation between anion−π and cation−π interactions, halogen bonds are often described as the underrecognized counterpart of hydrogen bonds.[40] They originate from the so-called σ hole, an electron-poor area that appears on "top" of electron-deficient halogen atoms, exactly opposite to the covalent bond to the withdrawing substituent. This localized σ hole makes halogen bonds highly directional, characterized by a bond angle of 180° at the halogen atom. Such a strict, linear directionality contrasts sharply to the almost "directionless" "π holes", i.e., the much larger cluster of multiple shallow local minima on π-acidic surfaces that accounts for anion−π interactions.[24] These complementary characteristics of σ and π holes determine their respective advantages in functional systems. Compared to hydrogen-bond donors, halogen-bond donors are not only of comparable in strength and better in directionality, they are also more hydrophobic. This property identifies halogen bonds as ideal to operate in nonpolar solvents and lipid bilayer membranes.[41]

Compared to anion−π interactions, halogen bonds are much older, much better understood and much more used. Many examples for self-organization and anion binding with halogen bonds exist in solid, liquid and gas phase.[40] Moreover, halogen bonds have been integrated into self-assembled supramolecular systems such as rotaxanes,[19] catenanes, foldamers,[42] capsules,[43] gels, fibrils, and so on.[40] Molecular recognition with halogen bonds is present in biology—tyroxine hormones and beyond—and extensively used in medicinal chemistry.[44] Anion transport with halogen bonds has been realized recently for monomers, cyclic oligomers and linear, membrane-spanning oligomers.[41] The discovery of trifluoroiodomethane as smallest possible organic anion transporter, one carbon only, a gas at room temperature, nicely illustrates the power of halogen bonds in lipid bilayer membranes.

**3.1. Catalysis with Halogen Bonds.** Several pioneering examples for halogen bonds in catalysis exist. The topic has been launched in 2008 with the hydrogen-transfer reduction of quinolone derivatives including **47** to secondary amines **48** (Figure 10).[12] Originally, simple fluorinated alkyl iodides **49** were used to activate acceptor **47** with a Hantzsch ester **50** (**TS12**). Later on, more powerful, divalent, cationic halogen-bond donors such as **51** were introduced to catalyze the same reaction as well as the general transfer hydrogenation of imines.[13]

Carbon−carbon bond formation with halogen bonds was achieved with a Diels−Alder reaction between cyclopentadiene **52** and enone **53** to give the bicyclic ketone **54** (Figure 11).[14] Halogen bonds from the divalent and cationic donors **55** to the carbonyl lone pairs were expected to activate dienophile **53**. This and several similar, also more advanced (bis)-halobenzimidazolium catalysts have been explored extensively
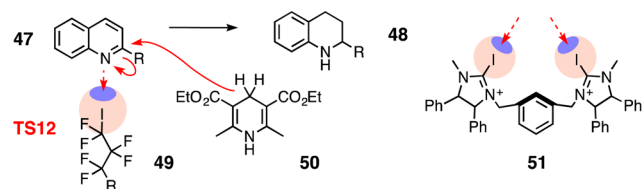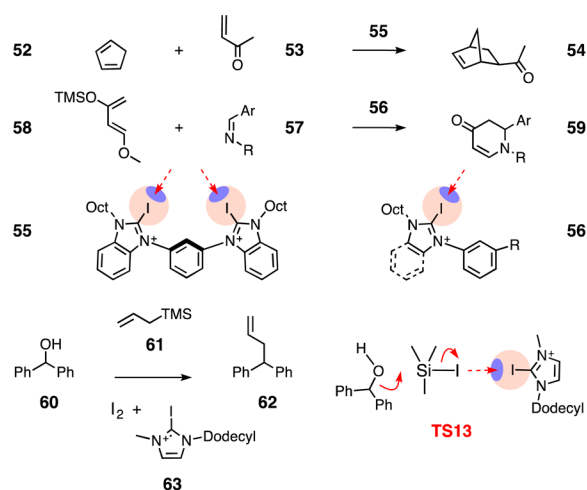
**Figure 11.** Recent examples for catalysis with halogen bonds include Diels−Alder reactions between dienes **52/58** and dienophiles **53/57**, respectively, and the more complex alkylation of **60**.

for anion-binding catalysis of the model reaction between 1-chloroisochroman **40** and silyl enol ether **41** (Figure 8).[15] Halogen-bond catalysis of a similar Diels−Alder reaction has been accomplished with catalyst **56** (Figure 11).[16] In this version, imine **57** is activated by halogen bonds to react with the Danishevsky diene **58** and afford heterocycle **59** after the elimination of methanol.

A more challenging example for halogen bonds in catalysis is the coupling of alcohols **60** with organosilanes **61** to afford alkene **62** in the presence of molecular iodine.[17] Catalyst **63** has been proposed to activate the iodide leaving group on the iodosilane intermediate by halogen bonding, which in turn is thought to cause the elimination of the hydroxide from substrate **60** (**TS13**, Figure 11). Contrary to the 5 years younger anion−π catalysis, several other examples exist already for halogen-bond catalysis. They include early Ritter-type reactions,[45] elegant semipinacol rearrangements,[46] and the ring-opening polymerization of L-lactide into poly(L-lactide)s.[47]

Asymmetric halogen-bond catalysis remains challenging. As far as biological systems are concerned, halogen bonds have been explored in the oxyanion hole of ketosteroid isomerase. However, the results were disappointing, either because the donors used were too weak or the bond angle was incorrect, i.e., ≪180°.[48]

**3.2. Halogen Bonds in Templated Transformations.** Templation by halogen bonds has been the key for the synthesis of poly(diiododiacetylene)s **64** (Figure 12).[18] This conjugated polymer is of interest because it contains only carbons and iodines and promises access to new ordered forms of carbon by removal of the iodines. Poly(diacetylene)s in general are accessible by topochemical polymerization of butadiynes in ordered materials, often solids. For the synthesis of poly(diiododiacetylene)s **64**, co-crystals **65** composed of diiodobutadiyne **66** and self-organizing halogen-bond donors such as bis(pyridyl)oxalimide **67** were grown. Whereas the common initiation of topochemical polymerization with light was ineffective, the crystals were found to gradually change color under pressure. Brownish color at 3 GPa indicated incomplete polymerization. At 6 GPa and more, the crystals turned dark blue. The possibility to remove templates such as **67** and isolate and study pure poly(diiododiacetylenes) **64** seems to exist. This example is important also because polymer

**Figure 10.** Initial studies on catalysis with halogen bonds focused on hydrogenation of **47**. The σ holes on iodine atoms are indicated blue on red.
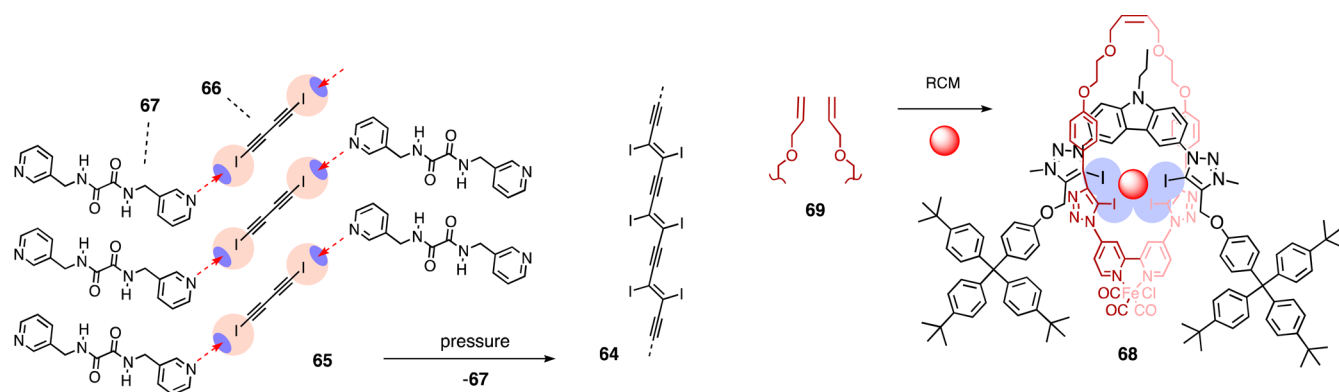
**Figure 12.** Synthetic access to conjugated polymers **64** composed of carbons and iodines and to anion-binding rotaxane **68** (blue circles, halogen-bond donors; red circles, anions) requires templation by halogen bonds (RCM = ring-closing metathesis).

**64** with all its promising structure, properties, and perspectives could not be obtained without templation from halogen bonds.

Other examples for transformations templated by halogen bonds include the synthesis of several rotaxanes and catenanes with interesting structures and functions, mostly anion binding.[40] An excellent example of this series is the synthesis of rotaxane **68** from acyclic substrate **69** by ring-closing olefin metathesis in the presence of anions (Figure 12).[19]

## 4. CHALCOGEN BONDS AT WORK

Like halogen bonds, chalcogen bonds originate from $\sigma$ holes.[24,49] Directed by the $\sigma$ holes opposite to the covalent bond, halogen bonds are linear. The $\sigma$ holes of electron-deficient, bivalent sulfur atoms are also opposite to each covalent bond. As a result, they appear on the side of the sulfur atom, just next to the other covalent bond (Figure 13). The resulting small bond angle has perhaps discouraged the use of intermolecular chalcogen bonds in the design of functional systems. Intramolecular non-covalent sulfur interactions, however, find broad use for conformational control. Examples reach from drug design in medicinal chemistry to the materials sciences.[49] Most common are 1,4, 1,5, and 1,6 O···S and N···S interactions with sulfur atoms in aromatic heterocycles, particularly thiazoles and thiophenes, serving as chalcogen-bond donors.

**4.1. Catalysis with Chalcogen Bonds.** Asymmetric acyl transfer is one of the few examples for chalcogen bonds in catalysis.[20] The bicyclic isothiourea **70** was shown to resolve racemic secondary benzyl alcohols **71** by stereoselective acylation, yielding ester **72** and leaving enantioenriched substrate **73** behind (Figure 13). As with standard catalysts such as DMAP or DBU, anhydrides like Ac$_2$O first acylate the catalyst **70**. In the acylated intermediate in **TS14**, an intramolecular 1,5 S···O bond from the endocyclic donor is decisive to orient the carbonyl for stereoselective addition. The approach of benzylalcohol **71** is controlled by $\pi-\pi$ interactions with the aromatic rings in the catalyst and steric repulsion from the phenyl substituent. Amidine analogues and the removal of the aromatic group both decrease stereoselectivity significantly. Intramolecular 1,5 chalcogen bonds were further considered to account for stereoselectivity of $\beta$-lactonizations and Michael additions.[50]

To preorganize photochromic cyclization with an intramolecular, planarizing 1,4 N···S chalcogen bond, two thiazoles were introduced in **74**.[21] By UV irradiation, crystals turned blue, whereas the thiophene analogues were not photochromic.
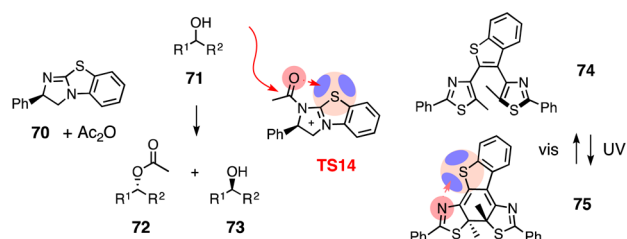


**Figure 13.** Catalysis with chalcogen bonds. Examples include stereoselective acylation with bicyclic isothiourea **70** and photochromic cyclization of thiazoles **74**. The $\sigma$ holes on endocyclic sulfurs are indicated blue on red.

The quantum yield of the photocyclization into the planar **75** in the nonpolar hexane was quantitative, whereas the thiophene analogues without chalcogen bonds performed with 49% only.

**4.2. Sensing with Chalcogen Bonds.** The planarization of conductive polymers with intramolecular chalcogen bonds is extensively used in the materials sciences.[51] Because of its use in organic solar cells, PEDOT might be the most popular example. Planarizing 1,5 O···S interactions are also expected to contribute to the properties of NDIs with sulfides in the core, including anion−$\pi$ catalysts **31** and **35** (Figures 6 and 7).[6,7] For sensing applications, the control of the planarity of polythiophenes has been maximized with a combination of attraction to and repulsion from "chalcogenic" $\sigma$ holes (Figure 14).[22] In solution, "chalcogen−hole repulsion" between the
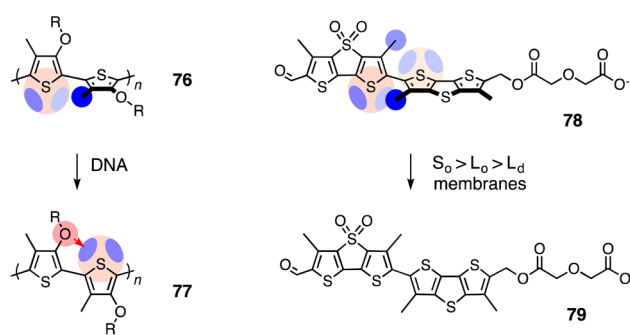


**Figure 14.** Sensing with chalcogen−hole attraction and repulsion. Examples include DNA sensing with twisted polythiophenes **76** and planarizable push−pull probes **78** as mechanosensitive membrane probes. The $\sigma$ holes on endocyclic sulfur atoms are indicated blue on red, chalcogen-bond acceptors in red, chalcogen−hole repulsion in blue.

endocyclic sulfur and the methyl substituents in polythiophene **76** dominates. Twisted out of conjugation, this deplanarization results in yellow colored polymers. Planarization is supported by the complementary chalcogen bond between the sulfur donors and the alkoxy substituents. Fully planarized, polymers **77** have bright red color. This change in color upon planarization was of interest for sensing applications. To nonspecifically bind to DNA, the alkoxy substituents were equipped with imidazolium cations. In the presence of both single- and double-stranded DNA, the yellow sensors **76** turned red, presumably due to planarization into the conformer **77**.

The concept of planarizable push—pull probes has been introduced to create mechanosensitive membrane probes.[23] For high mechanosensitivity and long fluorescent lifetime, two thiophenes each were bridged with a "sulfide" for the donor and a "sulfone" for the acceptor in push—pull mechanophore **78**. The highly fluorescent dithienothiophene S,S-dioxide was further supported by an aldehyde acceptor. Deplanarization of the push—pull mechanophore was achieved by "chalcogen—hole repulsion" between endocyclic donors and exocyclic methyls. A negative charge was attached for delivery and oriented partitioning into lipid bilayer membranes. Consistent with planarization into high-energy conformer **79** in confined space, the excitation maximum shifted up to 80 nm to the red in response to increasing order in the membrane, from liquid-disordered ($L_d$) to liquid- ($L_o$) and solid-ordered phase ($S_o$). Unchanged emission maxima confirmed that chalcogenic ground-state twisting of push—pull mechanophores provides conceptually new probes that are unrelated to TICT rotors or solvatochromic dyes. In mixed membranes of giant unilamellar vesicles, the different domains could be imaged with the same probe, more disordered ones with twisted probes **78**, excited at shorter wavelength, and more ordered ones with planarized probes **79**, excited at longer wavelength.

## 5. CONCLUDING REMARKS

The objective of this Perspective was to elaborate, in a comparative manner, on the recently emerging interest to integrate unorthodox interactions into functional systems. Emphasis was on ongoing progress toward catalytic systems that operate with $\pi$-hole and $\sigma$-hole interactions, i.e., anion—$\pi$ interactions, halogen bonds and chalcogen bonds. The charge-inverted cation—$\pi$ catalysis was added to this list because, although important in biology, it remains almost as underexplored in chemistry as the complementary anion—$\pi$ catalysis. Most functional systems operating with unorthodox noncovalent interactions that have been realized so far focus on conceptual innovation rather than practical use. These priorities are fully appropriate, even essential at this stage. However, the rapid growth of asymmetric ion-pairing catalysis has nicely illustrated how already the clever use of orthodox interactions can rapidly change a field to a quite remarkable extent.[52] Considering these attractive perspectives, the next milestones will concern *processes that are important but cannot be realized without* unorthodox interactions. This general objective is true not only for catalysis but also for other functions mentioned throughout the text, including self-assembly, templation, sensing, transport, and so on. As elaborated in this Perspective, pioneering examples in this direction, i.e., toward unorthodox interactions that achieve the otherwise unachievable, already exist. They encourage high expectations.

## ■ AUTHOR INFORMATION

**Corresponding Author**
*Stefan.Matile@unige.ch

**Present Address**
†Y.Z.: Institute of Polymers, ETH Zurich, Switzerland, and Qingdao University of Science and Technology, China

**Notes**
The authors declare no competing financial interest.

## ■ REFERENCES

(1) Knowles, R. R.; Lin, S.; Jacobsen, E. N. *J. Am. Chem. Soc.* **2010**, *132*, 5030−5032.
(2) Zhang, Q.; Tiefenbacher, K. *Nat. Chem.* **2015**, *7*, 197−202.
(3) Zhao, C.; Toste, F. D.; Raymond, K. N.; Bergman, R. G. *J. Am. Chem. Soc.* **2014**, *136*, 14409−14412.
(4) Holland, M. C.; Paul, S.; Schweizer, W. B.; Bergander, K.; Mück-Lichtenfeld, C.; Lakhdar, S.; Mayr, H.; Gilmour, R. *Angew. Chem., Int. Ed.* **2013**, *52*, 7967−7971.
(5) Zhao, Y.; Domoto, Y.; Orentas, E.; Beuchat, C.; Emery, D.; Mareda, J.; Sakai, N.; Matile, S. *Angew. Chem., Int. Ed.* **2013**, *52*, 9940−9943.
(6) Zhao, Y.; Benz, S.; Sakai, N.; Matile, S. *Chem. Sci.* **2015**, *6*, 6219−6223.
(7) Zhao, Y.; Cotelle, Y.; Avestro, A.-J.; Sakai, N.; Matile, S. *J. Am. Chem. Soc.* **2015**, *137*, 11582−11585.
(8) Berkessel, A.; Das, S.; Pekel, D.; Neudörfl, J.-M. *Angew. Chem., Int. Ed.* **2014**, *53*, 11660−11664.
(9) He, Q.; Ao, Y.-F.; Huang, Z.-T.; Wang, D.-X. *Angew. Chem., Int. Ed.* **2015**, *54*, 11785−11790.
(10) Schneebeli, S. T.; Frasconi, M.; Liu, Z.; Wu, Y.; Gardner, D. M.; Strutt, N. L.; Cheng, C.; Carmieli, R.; Wasielewski, M. R.; Stoddart, J. F. *Angew. Chem., Int. Ed.* **2013**, *52*, 13100−13104.
(11) Faraldos, J. A.; Antonczak, A. K.; Gonzalez, V.; Fullerton, R.; Tippmann, E. M.; Allemann, R. K. *J. Am. Chem. Soc.* **2011**, *133*, 13906−13909.
(12) Bruckmann, A.; Pena, M. A.; Bolm, C. *Synlett* **2008**, *2008*, 900−902.
(13) He, W.; Ge, Y.-C.; Tan, C.-H. *Org. Lett.* **2014**, *16*, 3244−3247.
(14) Jungbauer, S. H.; Walter, S. M.; Schindler, S.; Rout, L.; Kniep, F.; Huber, S. M. *Chem. Commun.* **2014**, *50*, 6281−6284.
(15) Jungbauer, S. H.; Huber, S. M. *J. Am. Chem. Soc.* **2015**, *137*, 12110−12120.
(16) Takeda, Y.; Hisakuni, D.; Lin, C.-H.; Minakata, S. *Org. Lett.* **2015**, *17*, 318−321.
(17) Saito, M.; Tsuji, N.; Kobayashi, Y.; Takemoto, Y. *Org. Lett.* **2015**, *17*, 3000−3003.
(18) Wilhelm, C.; Boyd, S. A.; Chawda, S.; Fowler, F. W.; Goroff, N. S.; Halada, G. P.; Grey, C. P.; Lauher, J. W.; Luo, L.; Martin, C. D.; Parise, J. B.; Tarabrella, C.; Webb, J. A. *J. Am. Chem. Soc.* **2008**, *130*, 4415−4420.
(19) Mullaney, B. R.; Thompson, A. L.; Beer, P. D. *Angew. Chem., Int. Ed.* **2014**, *53*, 11458−11462.
(20) Birman, V. B.; Li, X. *Org. Lett.* **2006**, *8*, 1351−1354.
(21) Fukumoto, S.; Nakashima, T.; Kawai, T. *Angew. Chem., Int. Ed.* **2011**, *50*, 1565−1568.
(22) Ho, H.-A.; Najari, A.; Leclerc, M. *Acc. Chem. Res.* **2008**, *41*, 168−178.

(23) Dal Molin, M.; Verolet, Q.; Colom, A.; Letrun, R.; Derivery, E.; Gonzalez-Gaitan, M.; Vauthey, E.; Roux, A.; Sakai, N.; Matile, S. *J. Am. Chem. Soc.* **2015**, *137*, 568−571.

(24) Bauzà, A.; Mooibroek, T. J.; Frontera, A. *ChemPhysChem* **2015**, *16*, 2496−2517.

(25) (a) Giese, M.; Albrecht, M.; Rissanen, K. *Chem. Rev.* **2015**, *115*, 8867−8895. (b) Chifotides, H. T.; Dunbar, K. R. *Acc. Chem. Res.* **2013**, *46*, 894−906. (c) Ballester, P. *Acc. Chem. Res.* **2013**, *46*, 874−884. (d) Frontera, A.; Gamez, P.; Mascal, M.; Mooibroek, T. J.; Reedijk, J. *Angew. Chem., Int. Ed.* **2011**, *50*, 9564−9583. (e) Salonen, L. M.; Ellermann, M.; Diederich, F. *Angew. Chem., Int. Ed.* **2011**, *50*, 4808−4842.

(26) Wang, D.-X.; Wang, M.-X. *Chimia* **2011**, *65*, 939−943.

(27) Schneider, H.-J.; Werner, F.; Blatter, T. *J. Phys. Org. Chem.* **1993**, *6*, 590−594.

(28) Gorteau, V.; Bollot, G.; Mareda, J.; Perez-Velasco, A.; Matile, S. *J. Am. Chem. Soc.* **2006**, *128*, 14788−14789.

(29) Dawson, R. E.; Hennig, A.; Weimann, D. P.; Emery, D.; Ravikumar, V.; Montenegro, J.; Takeuchi, T.; Gabutti, S.; Mayor, M.; Mareda, J.; Schalley, C. A.; Matile, S. *Nat. Chem.* **2010**, *2*, 533−538.

(30) Wendt, K. U.; Schulz, G. E.; Corey, E. J.; Liu, D. R. *Angew. Chem., Int. Ed.* **2000**, *39*, 2812−2833.

(31) Stauffer, D. A.; Barrans, R. E., Jr.; Dougherty, D. A. *Angew. Chem., Int. Ed. Engl.* **1990**, *29*, 915−918.

(32) Zhang, Q.; Tiefenbacher, K. *J. Am. Chem. Soc.* **2013**, *135*, 16213−16219.

(33) Hart-Cooper, W. M.; Clary, K. N.; Toste, F. D.; Bergman, R. G.; Raymond, K. N. *J. Am. Chem. Soc.* **2012**, *134*, 17873−17876.

(34) Ahrendt, K. A.; Borths, C. J.; MacMillan, D. W. C. *J. Am. Chem. Soc.* **2000**, *122*, 4243−4244.

(35) Yamada, S.; Fossey, J. S. *Org. Biomol. Chem.* **2011**, *9*, 7275−7281.

(36) Zhao, Y.; Beuchat, C.; Mareda, J.; Domoto, Y.; Gajewy, J.; Wilson, A.; Sakai, N.; Matile, S. *J. Am. Chem. Soc.* **2014**, *136*, 2101−2111.

(37) (a) Miros, F. N.; Zhao, Y.; Sargsyan, G.; Pupier, M.; Besnard, C.; Beuchat, C.; Mareda, J.; Sakai, N.; Matile, S. *Chem. - Eur. J.* **2016**, *22*, 2648−2657. (b) Cotelle, Y.; Benz, S.; Avestro, A.-J.; Ward, T. R.; Sakai, N.; Matile, S. *Angew. Chem., Int. Ed.* **2016**, DOI: 10.1002/anie.201600831.

(38) (a) Mitra, M.; Manna, P.; Seth, S. K.; Das, A.; Meredith, J.; Helliwell, M.; Bauzá, A.; Choudhury, S. R.; Frontera, A.; Mukhopadhyay, S. *CrystEngComm* **2013**, *15*, 686−696. (b) Rensing, S.; Arendt, M.; Springer, A.; Grawe, T.; Schrader, T. *J. Org. Chem.* **2001**, *66*, 5814−5821. (c) Orner, B. P.; Salvatella, X.; Sánchez Quesada, J.; De Mendoza, J.; Giralt, E.; Hamilton, A. D. *Angew. Chem., Int. Ed.* **2002**, *41*, 117−119.

(39) (a) Fujisawa, K.; Beuchat, C.; Humbert-Droz, M.; Wilson, A.; Wesolowski, T. A.; Mareda, J.; Sakai, N.; Matile, S. *Angew. Chem., Int. Ed.* **2014**, *53*, 11266−11269. (b) Fujisawa, K.; Humbert-Droz, M.; Letrun, R.; Vauthey, E.; Wesolowski, T. A.; Sakai, N.; Matile, S. *J. Am. Chem. Soc.* **2015**, *137*, 11047−11056.

(40) (a) Cavallo, G.; Metrangolo, P.; Milani, R.; Pilati, T.; Priimagi, A.; Resnati, G.; Terraneo, G. *Chem. Rev.* **2016**, DOI: 10.1021/acs.chemrev.5b00484. (b) Gilday, L. C.; Robinson, S. W.; Barendt, T. A.; Langton, M. J.; Mullaney, B. R.; Beer, P. D. *Chem. Rev.* **2015**, *115*, 7118−7195. (c) Beale, T. M.; Chudzinski, M. G.; Sarwar, M. G.; Taylor, M. S. *Chem. Soc. Rev.* **2013**, *42*, 1667−1680.

(41) Vargas Jentzsch, A.; Matile, S. *J. Am. Chem. Soc.* **2013**, *135*, 5302−5303.

(42) You, L.-Y.; Chen, S.-G.; Zhao, X.; Liu, Y.; Lan, W.-X.; Zhang, Y.; Lu, H.-J.; Cao, C.-Y.; Li, Z.-T. *Angew. Chem., Int. Ed.* **2012**, *51*, 1657−1661.

(43) Sarwar, M. G.; Ajami, D.; Theodorakopoulos, G.; Petsalakis, I. D.; Rebek, J. *J. Am. Chem. Soc.* **2013**, *135*, 13672−13675.

(44) Wilcken, R.; Zimmermann, M. O.; Lange, A.; Joerger, A. C.; Boeckler, F. M. *J. Med. Chem.* **2013**, *56*, 1363−1388.

(45) Walter, S. M.; Kniep, F.; Herdtweck, E.; Huber, S. M. *Angew. Chem., Int. Ed.* **2011**, *50*, 7187−7191.

(46) Tsuji, N.; Kobayashi, Y.; Takemoto, Y. *Chem. Commun.* **2014**, *50*, 13691.

(47) Coulembier, O.; Meyer, F.; Dubois, P. *Polym. Chem.* **2010**, *1*, 434−437.

(48) Kraut, D. A.; Churchill, M. J.; Dawson, P. E.; Herschlag, D. *ACS Chem. Biol.* **2009**, *4*, 269−273.

(49) Beno, B. R.; Yeung, K.-S.; Bartberger, M. D.; Pennington, L. D.; Meanwell, N. A. *J. Med. Chem.* **2015**, *58*, 4383−4438.

(50) Leverett, C. A.; Purohit, V. C.; Romo, D. *Angew. Chem., Int. Ed.* **2010**, *49*, 9479−9483.

(51) Roncali, J.; Blanchard, P.; Frère, P. *J. Mater. Chem.* **2005**, *15*, 1589−1610.

(52) (a) Lacour, J.; Moraleda, D. *Chem. Commun.* **2009**, *45*, 7073−7089. (b) Mahlau, M.; List, B. *Angew. Chem., Int. Ed.* **2013**, *52*, 518−533.